



HAL
open science

Decadal effects of solid industrial wastes on the coastal environment: Gulf of Gabes (Tunisia, Southern Mediterranean Sea) as an example

Radhouan El Zrelli, Lotfi Rabaoui, Mohsen Ben Alaya, Sylvie Castet, Cyril Zouiten, Nejla Bejaoui, Pierre Courjault-Radé

► **To cite this version:**

Radhouan El Zrelli, Lotfi Rabaoui, Mohsen Ben Alaya, Sylvie Castet, Cyril Zouiten, et al.. Decadal effects of solid industrial wastes on the coastal environment: Gulf of Gabes (Tunisia, Southern Mediterranean Sea) as an example. *Estuarine, Coastal and Shelf Science*, 2019, 224, pp.281 - 288. <10.1016/j.ecss.2019.04.021>. <hal-03486959>

HAL Id: hal-03486959

<https://hal.science/hal-03486959v1>

Submitted on 20 Dec 2021

HAL is a multi-disciplinary open access archive for the deposit and dissemination of scientific research documents, whether they are published or not. The documents may come from teaching and research institutions in France or abroad, or from public or private research centers.

L'archive ouverte pluridisciplinaire **HAL**, est destinée au dépôt et à la diffusion de documents scientifiques de niveau recherche, publiés ou non, émanant des établissements d'enseignement et de recherche français ou étrangers, des laboratoires publics ou privés.



Distributed under a Creative Commons CC BY-NC 4.0 - Attribution - Non-commercial use - International License

1 **Decadal effects of solid industrial wastes on the coastal environment: Gulf of Gabes**
2 **(Tunisia, Southern Mediterranean Sea) as an example**

3
4 Radhouan El Zrelli ^{(1,2)*}, Lotfi Rabaoui ^(3,4), Mohsen Ben Alaya ⁽⁵⁾, Sylvie Castet ⁽¹⁾, Cyril
5 Zouiten ⁽¹⁾, Nejla Bejaoui ⁽²⁾ and Pierre Courjault-Radé ⁽¹⁾

6
7 ⁽¹⁾ Géosciences Environnement Toulouse (GET), Université de Toulouse, UMR 5563
8 CNRS/UPS/IRD/CNES, 14 Avenue Edouard Belin, 31400 Toulouse, France

9 ⁽²⁾ Institut National Agronomique de Tunis (INAT), Université de Carthage, 43 Avenue
10 Charles Nicolle, 1082 Tunis Maharajène, Tunisia

11 ⁽³⁾ Marine Studies Section, Center for Environment and Water, King Fahd University of
12 Petroleum and Minerals, Dhahran, Saudi Arabia

13 ⁽⁴⁾ University of Tunis El Manar, Faculty of Science of Tunis, Research Unit of Integrative
14 Biology and Evolutionary and Functional Ecology of Aquatic Systems, University
15 Campus, 2092 Tunis, Tunisia

16 ⁽⁵⁾ Laboratoire des Matériaux Utiles (LMU), Institut de Recherche et d'Analyse Physico-
17 Chimique, Pôle Technologique Sidi Thabet, 2020 Ariana, Tunisia

18
19 * Corresponding Author: Radhouan El Zrelli (Email: radhouan.elzrelli@gmail.com / Mobile:
20 +33649831055)

34 **Abstract**

35 The present work examines the different types of solid effluents dumped in the coastal
36 environment from Gabes phosphate fertilizer plants, describes their coastal repartition and
37 assesses their long-term environmental impacts. Scanning Electron Microscopy analysis of
38 collected beach sediment samples showed that these wastes consist of phosphogypsum,
39 fluorapatite (phosphate ore grains), smokey quartz, calcite, fluorite, calcite-Mg, apatite, pyrite,
40 albite, sphalerite-Cd-U, fluorosilicates, sulfur dross and spent catalysts. Using fluorapatite as a
41 mineralogical marker of the coastal spatial distribution of industrial wastes, solid effluents
42 were found to carry bottom and/or suspended loads with a coastal transport limited at
43 Essorag Wadi, ~ 10 km south from the industrial emissary. Phosphogypsum which is the
44 main solid effluent was found to be completely dissolved in the seawater. The main decadal
45 consequences of solid effluents on the coast were found to be the following: local
46 disappearance of *Posidonia oceanica* seagrass, formation of an azoic benthic zone between
47 Gabes and Ghannouche ports, gradual fattening of the beach, shoreline advancement,
48 formation of a belt of coastal dunes, mouth clogging of coastal streams and formation of
49 coastal lakes.

50

51 **Keywords:** Anthropogenic pressure; Solid wastes; Coastal modifications; Tunisian Chemical
52 Group; Phosphates; Fluorapatite.

53

54

55

56

57

58

59

60

61

62

63

64

65

66

67 1. Introduction

68 Due to the increasing urbanization and industrialization of the coasts, huge quantities of
69 industrial/solid wastes end in the marine environment, leading to its deterioration (Tosic et al.,
70 2018) and consequently to various socio-economic impacts. For example, it is estimated that
71 the Mediterranean Sea receives yearly $650 \cdot 10^6$ t of sewages, $129 \cdot 10^3$ t of mineral oil, $60 \cdot 10^3$ t
72 of mercury, $36 \cdot 10^3$ t of phosphates and $3.8 \cdot 10^2$ t of lead (UNEP, 2012). In addition to the
73 environmental and health issues related to solid waste disposal in the marine environment,
74 solid wastes can be responsible for a range of economic impacts on marine and coastal
75 activities reducing the economic benefits derived from them (Newman et al., 2015). In fact, in
76 the absence of a good management strategy, solid wastes, in particular industrial ones, can
77 impact the fragile coastal ecosystems, economic sectors such as tourism and fisheries and
78 even public health (Kindt, 1984; Alam and Ahmade, 2013; Groeneveld et al., 2018). Industrial
79 solid wastes are of particular concern because they may consist of various harmful pollutants
80 including heavy metals and radioelements which can deteriorate the marine life and flora
81 leading to the contamination, erosion and modification of the coast. Among the various
82 industrial solid wastes dumped in the Mediterranean marine environment, phosphogypsum
83 (PG; Perriñez, 2002) is an industrial radiochemical by-product of phosphoric acid production
84 which is environmentally hazardous and potentially harmful to human health (El Zrelli et al.,
85 2018a).

86 The Gulf of Gabes (GG) extends from Ras Kaboudia in the north to the Tunisian-Libyan
87 borders in the south (Fig. 1). It represents the widest continental shelf area in the
88 Mediterranean Basin, together with the North-Central Adriatic shelf, covering about 36.10^3
89 km^2 (Hattab et al., 2013; Halouani et al., 2016). The Gulf of Gabes is known to have very
90 large continental plateau with a very light slope, making the 200m isobath reachable at almost
91 250 km from the coastline (Seurat, 1934; Hattour and Ben Mustapha, 2013). GG had been
92 considered as one of the most productive Mediterranean regions (Abdou et al., 2016) and one
93 of the most important fishing zones (Papaconstantinou and Farrugio, 2000), with a variety of
94 fishing activities (Rabaoui et al., 2010; Hattab et al., 2011), due mainly to the largest area
95 covered by *Posidonia oceanica* seagrass beds that it used to host (De Gaillande, 1970; Batisse
96 and De Grissac, 1998; Hattour and Ben Mustapha, 2013). In spite of its various and important
97 ecological and economic services, the GG is currently considered as the most heavily polluted
98 Mediterranean marine area (El Zrelli et al., 2017). In particular, in its central part, various
99 anthropogenic factors are continuously exerting pressure on its natural habitats making them

100 very vulnerable. For instance, the central GG coastal area is the destination of various
101 industrial and domestic pollutants and wastes which have immensely contributed to the
102 destruction of its specific flora (e.g. *Posidonia oceanica*; Zaouali, 1993; El Zrelli et al.,
103 2017), fauna (Darmoul and Vitiello, 1980; Rabaoui et al., 2010, 2015; Ayadi et al., 2016; El
104 Kateb et al., 2016), as well as its sediments (Ayadi et al., 2014; El Zrelli et al., 2015; Rabaoui
105 et al., 2015; El Kateb et al., 2018) and seawater quality (Darmoul et al., 1980; Darmoul, 1988;
106 El Zrelli et al., 2018b; El Kateb et al., 2018). Among these different industrial wastes, solid
107 industrial effluents which are mainly represented by PG by-produced from the Tunisian
108 Chemical Group of Gabes (Groupe Chimique Tunisien, GCT), raise a major environmental
109 concern for the coastal habitats of central GG (Darmoul, 1988; Rabaoui et al., 2014; El Zrelli
110 et al., 2015; El Kateb et al., 2016). In fact, a daily average of $\sim 30 \cdot 10^3$ tons of untreated humid
111 PG (El Zrelli et al., 2017) and other unknown industrial wastes have been continuously
112 thrown, from the GCT in the central GG coastal area. These wastes are responsible of a clear
113 damage of the local marine environment, biodiversity loss and modification of the coast, since
114 the first observations of Darmoul et al. in 1976 (Darmoul et al., 1980). Thus, it is very
115 probable that these wastes have affected, along the last decades, the coastal landscape of
116 central GG at different levels. The present study was conducted for the first time within this
117 context and it aims at *i*) identifying the different types of solid industrial effluents discharged
118 in the marine environment, *ii*) describing their coastal spatial distribution and *iii*) assessing
119 their long-term effects on this area.

120

121 2. Materials and Methods

122 2.1. Sampling area, trenching and beach sediment sampling

123 In September/October 2014, 12 sedimentary coastal trenches were made at 10 sampling
124 stations spread at the transitional zone between the wrack line and the beach berm, between
125 the marine discharge of GCT (source) and Zarat Beach (Fig. 1). At the beginning of the study,
126 only one trench was realized at each station, but after the examination of the trenches done,
127 we decided to make 2 additional trenches in Chat Essalam in order to better understand and
128 confirm the distinguished sedimentary profile in this latter station. At each station, trenching
129 was aborted when reaching the water level, and hence the depth of the trenches varied from
130 0.65 (at Tebelbou) to > 2.20 m (at Chat Essalam). Systematically, after digging each trench,
131 one composite sediment sample (made by mixing three different samples) was collected from
132 each sediment layer observed in each trench. In total, 23 composite sediment samples were

133 collected with a rate of only 1 sample from each of the trenches done in LM, KT and ZT, 2
134 samples from each of the trenches in LG, CR, OG, CM, MT and TB, and 2 to 3 samples from
135 each of the trenches dug in Chat Essalam (i.e. CE1, CE2 and CE3) (Table 1; Fig. 1).

136 The study area was divided into 2 sectors:

- 137 • **Inter-harbour Sector:** located between the commercial harbor of Ghannouche in the
138 north and the fishing port of Gabes city in the south (Fig. 1). It extends along 2.5 km
139 between Legusir Wadi which is used as the industrial releases emissary of GCT and
140 Ennaten Wadi to the south (Fig. 1). It contains 2 stations (LG and CE) and is
141 characterised by relatively low hydrodynamic energy conditions (Gzam et al., 2016)
142 due of the influence of the structures of the two ports (El Zrelli et al., 2015).
- 143 • **Southern Sector:** located toward the south and is characterized by moderate energy
144 conditions (Gzam et al., 2016). It extends nearly along 30 km from the fishing port of
145 Gabes to Zarat Beach in the south (Fig. 1) This sector hosts the other 8 sampling
146 stations: CR, OG, CM, MT, TB, LM, KT and ZT (Fig. 1).

147

148 In addition to the 23 sediment samples collected from the ten sampling stations above-
149 mentioned, 2 additional sediment samples were taken directly from the littoral industrial
150 emissary of GCT. The first sample (E1) was taken at the level of the industrial canal bed
151 where the current is strong, in order to have the coarse fraction of the dumped industrial
152 wastes. However, the second sample (E2) is much finer because it comes from the delta of
153 industrial channel where the environment is less agitated (low hydrodynamics energy). These
154 2 additional samples were collected in order to identify the different types of industrial wastes
155 thrown from the coastal phosphate fertilizer factories of Gabes city. Collected sediment
156 samples were placed separately in sealed and clean polyethylene bags. In the laboratory,
157 samples were dried in an oven at 60°C for few days to a constant weight.

158

159 2.2. Mineralogical, morphological and granulometric characterization of beach sediments 160 and solid wastes.

161 The collected sediment samples were first observed under a binocular loupe in order to
162 determine their general characteristics (color, size, shape, etc.). After embedding the sediment
163 samples, polished sections were prepared and observed under a Scanning Electron
164 Microscopy (SEM; JEOL JSM 6360LV) coupled with an Energy Dispersive Spectroscopy
165 detector (EDS; SAHARA Silicon Drift Detector). The SEM-EDS analysis enabled to

166 determine the mineralogical, morphological and granulometric characteristics of each
167 sediment sample.

168

169 2.3. Sedimentological characterization of the beach area in the two sectors

170 Each of the two sectors defined herein was chosen to serve a well-defined purpose. The inter-
171 harbour sector was firstly used (i) to identify the different types of industrial wastes thrown
172 from the GCT factories because it shelters in its northern part the littoral channel of these
173 wastes. This sector is limited by the piers of the commercial and fishing harbours which trap a
174 large part of industrial wastes, making it the most affected area by these industrial discharges
175 (Ayadi et al., 2014; El Zrelli et al., 2015). Hence, this sector was defined (ii) to identify the
176 impacts of phosphate plant discharges on the coastal environment. Sediment samples
177 collected from the different layers of the trenches done in Chat Essalam station, were used to
178 assess the concentration of the inorganic phosphorus (P_{ing}), cadmium (Cd), Zinc (Zn),
179 Chromium (Cr), Copper (Cu), Mercury (Hg) and Lead (Pb). Elemental analyses were
180 conducted following the methodology described in El Zrelli et al. (2015).

181 Because of its location in the direction of PG marine dispersion (El Zrelli et al., 2015) and
182 hence in the direction of discharged solid wastes, the southern sector represents the ideal area
183 (iii) to determine the spatial limit of GCT solid wastes' sedimentary transport in central GG.

184

185 2.4. Spatial limitation of the coastal transport of industrial solid wastes

186 In order to spatially limit the littoral extension of sedimentary transport of GCT solid wastes,
187 the fluorapatite, one of the main insoluble minerals of phosphate ore grains dumped by the
188 coastal factories into the seawater of GG (present study), was used as a "mineralogical
189 marker" of industrial waste littoral transport. The choice of fluorapatite is also confirmed with
190 the study of Poizat (1970) which was conducted, before the setup of the phosphate fertilizer
191 plant (in 1972), on the analysis of GG coastal sediments and did not report the presence of this
192 mineral. For this purpose, we have used the optical and electronic microscopy to minutely
193 search the presence of this marker in the sediments from the southern zone in the direction of
194 transport of these industrial wastes (El Zrelli et al., 2015). We started with the southernmost
195 station (Zarat) towards the industrial wastes source. The principle of the method used is too
196 simple: the first southern station, where fluorapatite is found, represents the limit of industrial
197 wastes transport.

198

199 2.5. *Assessment of the long-term effects of PG industrial wastes on the central coastal area*
200 *of GG*

201 After several years of observation (1990-2018) and during many field campaigns carried out
202 in our study area (2013-2017), several field surveys were done with local habitants in order to
203 determine the coastal modifications since the beginning of solid wastes dumping in the littoral
204 environment (1972). For the same purpose, we have studied and compared several ancient
205 photos (since 1952), aerial (since 1949) and satellite images from different free sources (since
206 1984 from Google Earth and LandSat) of central part of GG.

207

208 **3. Results and discussion**

209 *3.1. Qualitative identification of different types of industrial solid wastes*

210 The SEM observation of two sediment samples collected from the bed (E1, coarse fraction)
211 and delta (E2, fine fraction) of the marine effluents, from the industrial discharges of Gabes
212 phosphate chemical complex, showed the presence of several types of minerals. The coarse
213 fraction (Fig. 2) consisted essentially of fluorapatite, smokey quartz, calcite, fluorite, sulfur
214 dross, spent catalysts (i.e. solid wastes produced during the process of sulfuric acid production
215 and composed mainly by C, O and Si), sphalerite-Cd-U (Fig. 3), apatite and fluorosilicates.
216 The fine fraction was found to be formed by phosphogypsum, smokey quartz, fluorapatite,
217 calcite-Mg, sphalerite-Cd, fluorite, pyrite and albite. The diversity of identified minerals
218 showed that GCT plants do not only throw PG wastes ($\sim 30 \cdot 10^3$ t/day of humid PG; El Zrelli et
219 al., 2017), but also phosphate ore grains and other untreated industrial solid wastes like sulfur
220 dross and used catalysts.

221 Historically speaking, the first studies on the environmental impacts of the GCT industrial
222 wastes on the Gabes Gulf reported liquid effluents as the only form of industrial wastes
223 discharged in the marine environment at the beginning of coastal industry (Darmoul et al.,
224 1980a and b; Darmoul, 1988). Along the decades following the setup of the phosphate
225 industry in Gabes coast, the industrial wastes have been intensified and diversified. This has
226 been accentuated with the absence of priorities of marine environment protection in the
227 seventies and development of GCT industries, leading to increase the anthropogenic pressure
228 on the coastal environment which has become the receiving area in which end all generated
229 wastes. Compared with other coastal areas hosting phosphate industries such as Sfax (Tunisia;
230 Gargouri et al., 2010; Naifar et al., 2018), Huelva (Spain; Morillo et al., 2004; Pérez-López et
231 al., 2011), El Jadida (Morocco; Gaudry et al., 2007), Kpémé (Togo; Bawa et al., 2006) and

232 Batroun (Lebanon; Fakhri et al., 2008), the observation of industrial solid wastes, including
233 phosphate ores, spent catalysts and sulfur dross, being discharged in Gabes coastal waters was
234 reported only during this study.

235

236 3.2. Sedimentological characterization of different beach layers

237 The examination of the twelve beach trenches carried out in the studied area allowed to
238 distinguish 4 successive layers, L1, L2, L3 and L4, in the inter-harbour area and only one
239 contaminated layer (L_S) in southern sector. They are sedimentologically and mineralogically
240 heterogeneous (Figs. 4 & 5; Table 2). The L1 layer was found throughout the study area
241 (Zone 1, 2 and 3; Fig. 5) and consisted of the regional white fine-grained sand and was found
242 to be mineralogically uncontaminated with the presence of quartz, calcite and some opaque
243 grains essentially represented by zircon, iron oxides and titanomagnetite minerals (Table 2).
244 The L2, L3 and L4 layers are exclusively located in the inter-harbor area (Fig. 4; Zone 1 in
245 Fig. 5) and were found to be characterized by coarser particle size and darker color than the
246 bottom layer L1 (Table 2). In addition, these last 3 layers are contaminated because of their
247 enrichment with several minerals of industrial origin such as fluorapatite, calcite-Mg,
248 sphalerite-Cd-U, fluorosilicates and some sulfur dross (SM-Fig. 1); these latter were not found
249 in L1 (see more details in Table 2). Besides, it is also important to note that L4 layer could be
250 considered as a typical industrial wastes layer, formed by almost only phosphate ore grains
251 (Table 2). Indeed, even with naked eyes, this layer was found to be distinguished from the
252 other two "mineralogically" contaminated layers (L2 and L3) by the dominance of phosphate
253 raw minerals, mainly fluorapatite, which gave it the dark brown to blackish color. Finally, the
254 L_S layer is spatially limited in Zone 2 of the southern sector (Fig. 5) and is composed by fine-
255 sized sand grains and characterized with a greyish color, due to the presence of calcite-Mg
256 (Table 2).

257 Fig. 5 shows the East-West (E-W) and North-South (N-S) interpretative diagrams of the
258 trench profiles found in our study area, showing the sequential organization of the different
259 layers already defined in Fig. 4 and described in Table 2.

260 The E-W section of Zone 1 (Fig. 5A) showed the occurrence of 3 main different phases of
261 industrial discharges (corresponding to the three layers L2, L3 and L4), since the set-up of the
262 phosphate fertilizer industry along the coast of Gabes (in 1972). These three layers are
263 simultaneously marked with their horizontal increase of grain size and their contents of
264 phosphate grains, in particular fluorapatite, from the base (L2) to the surface (L4). These

265 granulometric and mineralogical differences are related to the changes in industrial processes
266 and consequently the changes in the types of industrial wastes released. Within this context, it
267 is worth noting that the last industrial phase which corresponds to the surface layer, L4, was
268 found to be granulometrically, mineralogically and quantitatively the most important
269 compared to the two others phases (L2 and L3). Indeed, this last phase is the main phase
270 responsible for the various radical morphological changes seen at present, in particular in the
271 inter-harbor beach (Zone 1; Fig. 5; SM-Fig. 2). Figure 6 showed the variations of elements
272 (P_{ing} , Cd, Zn, Cr, Cu, Hg and Pb) concentrations analyzed in the sediment samples collected
273 from Chatt Essalam Beach layers. The concentrations of P_{ing} varied between 0.15 g kg^{-1} (in
274 L1) and 39.1 g kg^{-1} (in L3); those of Cd between 4 mg kg^{-1} (in L1) and 723 mg kg^{-1} (in L4).
275 The concentrations of Cr were found to vary from 10 mg kg^{-1} (in L1) to 57 mg kg^{-1} (in L4). In
276 the case of Cu, concentrations ranged between 2.2 mg kg^{-1} (in L1) and 6.4 mg kg^{-1} (in L4).
277 Regarding the concentrations of Hg, they varied from 0.011 mg kg^{-1} (in L1) and 0.026 mg kg^{-1}
278 (in L4). As for Pb, its concentrations ranged between 4.8 mg kg^{-1} (in L1) and 11.9 mg kg^{-1} (in
279 L2); those of Zn between 4.9 mg kg^{-1} (in L1) and 4732 mg kg^{-1} (in L4). In addition, the lowest
280 concentrations of all elements taken into consideration were recorded in the uncontaminated
281 layer L1; whereas the highest concentrations were found in the other three layers (L2, L3 and
282 L4; Fig. 3). The geochemical enrichment of these three latter (upper) layers is most likely due
283 to their 'mineralogical contamination' by the typical phosphate minerals mainly fluorapatite
284 and sphalerite-Cd (Sassi and Sassi, 1999).

285 As for the N-S section profile (Fig. 5D), it showed that the industrial impacts on the beach
286 environment are not only concentrated in the inter-harbor zone (Fig. 5A and D) but they are
287 also extended to southward-spreading (Zone 2; Fig.5B), with a very much lower amplitude. A
288 thin (up to 80 cm) dark-greyish contaminated layer (L_s) is found to overlay the regional
289 uncontaminated white sands. It ends at Essorag Wadi (Fig. 5D) thus marking the spatial limit
290 of coastal solid waste transport at this level (~10 km from the source).

291 Comparing between known phosphate industries in the Mediterranean Sea, the largest marine
292 releases of phosphogypsum are being dumped by the GCT plants of Gabes (~ $30 \cdot 10^3$ tons of
293 untreated humid PG; El Zrelli et al., 2017). For example, in Batroun region (North Lebanon),
294 only 950 t of PG are daily discharged in the sea (METAP/Tebodin, 1998) which represents
295 more than 30 times less than the quantities rejected in Gabes. In addition, the other insoluble
296 industrial wastes such as phosphate ores, sulfur dross and used catalysts are discharged only
297 in the coastal waters. All other phosphate industries do not follow the same practices adopted

298 by Gabes phosphate factories. These latter fractions (i.e. phosphate ores, sulfur dross and used
299 catalysts) cannot be dissolved in the seawater end are therefore washed on the coastal beaches
300 where they accumulate with years to form stratified layers with respect to the type of wastes
301 they form.

302

303 3.3. Spatial limitation of the solid industrial wastes impact on the central coastal area of 304 Gabes Gulf: Spatial repartition of fluorapatite mineral

305 Fluorapatite grains, the main mineral component of Tunisian phosphate ores, were used as the
306 mineralogical marker of the coastal spatial distribution of solid GCT wastes, since they
307 predominantly occur in all the contaminated layers of the inter-harbor (L2 to L4) and southern
308 (Corniche to Tebelbou sampling stations, L_s) sectors). Figure 7 showed the scanning electron
309 microscopy photos of some representative fluorapatite mineral grains from 3 stations: Legusir
310 (LG; the source of GCT solid wastes), Chatt Essalam (CE; the most impacted coastal zone)
311 and Tebelbou (TB; the limit of the presence of contaminated industrial layer L_s). These grains
312 are distinguished by different shapes and sizes, with respect to the sampling stations. The LG
313 fluorapatite grains (Fig. 7) are characterized by elongated shapes and large sizes (between
314 1050 and 1200 µm). However, in the two other stations (CE and TB), the fluorapatite grains
315 have almost the same spherical shape but with different sizes: CE fluorapatite grains ranging
316 between 600 and 800 µm are larger than those of TB fluorapatite grains (between 230 and
317 280µm). Within this context, each grain size may be associated with a specific mechanism of
318 transport (Wilcock et al., 2009) in a moderate hydrodynamic context like the study area of GG
319 (Maghrebi, 1995; Guillaumont et al., 1995; Hattour et al., 2010). Industrial emissary (LG)
320 fluorapatite is transported only in bed load by sliding and rolling or hopping according to
321 Wilcock et al. (2009). Two transport mechanisms are possible for the inter-harour sector
322 fluorapatite grains (Chatt Essalam): bed load and suspended load. Finally, the fluorapatite
323 mineral grains of the southern sector move exclusively in suspension with the seawater mass
324 along the southern-directed littoral drift (suspended load; Wilcock et al., 2009). This transport
325 mode may be added to another particular mode: the transport in colloidal suspension by the
326 PG foams (SM-Fig. 3). According to El Zrelli et al. (2019), PG foams can migrate far into the
327 marine environment (reaching tens of km) transporting with them small grains of fluorapatite
328 and depositing them after their mechanical collapse as shown in SM-Fig. 3. These results
329 showed that the sedimentary coastal transport of GCT solid wastes - essentially phosphates
330 grains – is limited spatially at the level of Essorag Wadi, at ~10 km far from their source.

331 Besides, it is worth noting that from Legusir to Zarat stations (~30 km), no trace of PG, the
332 main solid wastes of phosphoric acid factories, was detected except for the area located in
333 front of the industrial discharge delta. Hence, it is strongly suggested that PG is completely
334 dissolved in the seawater. This dissolution contributes enormously to the marine dispersion of
335 the polluting load of these radiochemical industrial wastes (El Zrelli et al., 2018a).

336 In other areas hosting phosphate industries such as Batroun (Lebanon), El Jadida (Morocco)
337 and Seine estuary (France; where PG discharges stopped in 1992), the environmental impacts
338 of the PG industrial wastes remain spatially limited (Fakhri et al., 2009, 2011; Simon et al.,
339 2000), contrary to what is being observed in Gabes. Various anthropogenic and natural factors
340 can explain the current status of the coastal area in GG. For instance, the important quantities
341 (~10.5.10⁶ t/year of humid PG; El Zrelli et al., 2017) and diversity of industrial discharges
342 (Fig. 2), spatial extension and low inclination of the continental shelf (Hattab et al., 2013;
343 Halouani et al., 2016; Hattour and Ben Mustapha, 2013) and the role played by harbors'
344 marine structures (Rabaoui et al., 2014; El Zrelli et al., 2015) act in synergy in order to
345 enlarge the spatial extent of the environmental impacts of the GCT discharges towards the
346 area located southern the discharge source (~ 10 km; Fig. 5).

347 348 3.4. Assessment of the long-term effects of solid wastes on the central coastal area of GG

349 The central coastal area of GG has known various geomorphological changes due to the huge
350 quantities of various solid industrial wastes (mainly PG) dumped by the GCT factories
351 directly in the sea. In fact, just few years after the beginning of the GCT marine discharges,
352 Darmoul (1988) observed a degradation of the *Posidonia oceanica* seagrass beds in front of
353 the industrial emissary. Various authors highlighted that this degradation is mainly due to the
354 effects of the untreated PG dumped in the coastal environment sea (Darmoul et al., 1980a;
355 Darmoul, 1988; Zaouali, 1993; El Zrelli et al., 2017). This industrial waste was also reported
356 to be responsible of other environmental consequences including the increase of water
357 turbidity (Darmoul et al., 1980a), chemical contamination of seawater (Darmoul et al., 1980a;
358 Kharroubi et al., 2012; El Zrelli et al., 2018b), destruction of the benthic community
359 (Darmoul et al., 1980a and b; Rabaoui et al., 2014, 2015; El Kateb et al., 2016, 2018; El Zrelli
360 et al., 2017) and silting up the seabed (Darmoul et al., 1980a; Zaouali, 1993). A recently-
361 conducted study confirmed the cumulative negative impact of PG on *P. oceanica* meadows
362 which disappeared -almost- completely from the study area, except for few small patches of
363 this plant still remaining at almost 6 km (~ few hundred meters after the CM station described

364 herein; Fig. 1) to the south of the PG emissary (El Zrelli et al., 2017). Consequently, an azoic
365 benthic zone was established in the coastal area between the two ports of Ghannouche and
366 Gabes, inter-harbor sector (SM-Fig. 4; Rabaoui et al., 2015). In all, the local disappearance of
367 *P. oceanica* seagrass can be considered as the major impact of GCT industrial marine
368 discharges, in particular because this endemic plant represents a key species in the coastal
369 ecosystem of GG (El Zrelli et al., 2017). Other serious changes caused by these industrial
370 wastes took also place in the central coastal area of GG leading to more accentuate the
371 degradation of the coastal habitat in this region. The surplus of industrial-derived coastal
372 sediments have gradually led to a "fattening" of Chatt Essalam Beach (SM-Fig. 5) from the
373 north to the south, in the direction of marine transport of industrial wastes (El Zrelli et al.,
374 2015). This phenomenon was, firstly, caused the advancement of the shoreline more than 200
375 meters in the northern part of this area, close to the GCT industrial emissary (SM-Fig. 6), with
376 the formation of a belt of some coastal dunes (SM-Fig. 7). The disappearance of an old coastal
377 building of a red tuna processing plant present until 2013 (SM-Fig. 8), could be an additional
378 proof of the beach flattening of the inter-harbor coastal area. In addition, the large quantities
379 of industrial wastes have gradually clogging the mouths of 2 coastal streams (SM-Fig. 9)
380 which has led to the formation of 2 small coastal lakes (Aouina and Ayatt lakes; SM-Fig. 10).
381 It is worth noting that the coastal installations of commercial and fishing harbors might most
382 likely play indirectly an essential role in the succession of these coastal modifications through
383 the entrapment of a large proportion of these industrial wastes in the inter-harbor area. This
384 can be confirmed with the Google Earth photo given in SM-Fig. 11, which showed that the
385 sediments of the inter-harbor sector have a dark black color; whereas those of the southern
386 area have a clear color.

387 The impacts of phosphate treatment industries on the coastal environment are known to differ
388 with respect to hydrodynamic and geomorphologic features. For example, in the Lebanese
389 coastal area of Batroun, the dumped PG discharges have affected the sediment quality leading
390 to the prevalence of fine fractions, decreased pH and oxidation reduction potential, and
391 increased inorganic phosphate concentrations (Fakhri et al., 2009, 2011). The latter authors
392 have also observed a strong shrinkage of meiofauna representation and higher chlorophyll *a*
393 concentrations in the sediments in the front of the PG emissary. Seawater quality was also
394 found to be affected by PG wastes through the increase in its pH, temperature and
395 orthophosphate concentrations (Fakhri et al., 2009, 2011). Similar impacts were also observed
396 in the Seine Estuary (France), decades after banning the PG discharges in the Seine River

397 (Simon et al., 2000; Chiffoleau et al., 2001). This leads to deduce that the environmental
398 impacts of PG releases observed in Gabes will most likely remain for decades, even if these
399 industrial effluents are stopped, and that the restoration of the coastal environment which has
400 been affected for decades (more than 50 years) will necessarily require a depollution phase of
401 the water and sediments, followed by a monitoring program at different levels (fauna, flora,
402 sediment, water...etc.). Moreover, the local regression/disappearance of *P. oceanica* seagrass
403 from the central area of Gabes Gulf, caused by PG discharges, is most likely the triggering
404 factor provoking, through a 'domino' effect, the other morphological impacts (SM-Fig. 4 to
405 SM-Fig. 10). In fact, *P. oceanica* naturally ensures the stability of sandy shores and seabed
406 (Maggi, 1973; Hattour and Ben Mustapha, 2013). Therefore, any future remediation program
407 of the marine environment in Gabes should begin with the introduction of this endemic
408 Mediterranean species which can help to restore the ecological balance of the GG ecosystem.

409

410 **4. Conclusions**

411 Summarizing, the present study showed that the solid industrial effluents are formed by
412 phosphogypsum, fluorapatite, smokey quartz, calcite, fluorite, calcite-Mg, apatite, pyrite,
413 albite, sphalerite-Cd-U, fluorosilicates, sulfur dross and spent catalysts. Essorag Wadi
414 represents the spatial limit of coastal sedimentary transport of the solid industrial wastes
415 (phosphate grains). One must note that phosphogypsum was found to be completely dissolved
416 in the seawater. Since the installation of the industrial complex in the coast of Gabes city in
417 1972, the coastal landscape has undergone several major modifications. The local extinction
418 of *P. oceanica* seagrass, installation of azoic benthic seabed in the inter-harbor area, gradual
419 fattening of beaches, advancement of the shoreline, formation of a costal dunes belt, clogging
420 of the coastal streams' mouths and formation of coastal lakes represent the main coastal
421 changes identified in this study. Based on these findings, a rapid intervention is necessarily
422 and urgently needed in order to allow the recovery of the impacted coastal habitats of central
423 Gabes Gulf. To ensure the success of any remediation plan of central GG, it is mandatory to
424 ban dumping all types of industrial discharges in the marine environment. Achieving the
425 restoration of Gabes Gulf environment cannot be done considering only this latter step. Other
426 steps should be also considered including the decontamination of the seabed and clean-up of
427 beaches. These measures will certainly help the re-appearance of locally-extinct taxa such as *P.*
428 *oceanica* which play the role of a key species in the Gulf of Gabes.

429

430 **Acknowledgments**

431 This study is dedicated to the memory of Nader Chkiwa (28.04.1986/08.08.2017), the ex-
432 president of the “Association de la Protection de l'Oasis de Chatt Sidi Abd Essalam”. The
433 authors would like to thank the editor and reviewer of the paper for their constructive
434 comments and suggestions which helped to improve the quality of the manuscript.

435

436 **References**

- 437 Abdou, K., Halouani, G., Hattab, T., Romdhane, M.S., Lasram, F.B.R., Le Loc'h F., 2016.
438 Exploring the potential effects of marine protected areas on the ecosystem structure of
439 the Gulf of Gabes using the Ecospace model. *Aquat. Living Resour* 29: 202.
- 440 Alam, P., Ahmade, K., 2013. Impact of solid waste on health and the environment. *J Sustain*
441 *Devel Green Econ* 2: 165-168.
- 442 Aminot, A., Le Guellec, A.M., Mauvais, J.L., 1986. Le fluorure en Baie de Seine. IFREMER,
443 Actes de colloques 4: 283-288.
- 444 Ayadi, N., Aloulou, F., Bouzid, J., 2014. Assessment of contaminated sediment by phosphate
445 fertilizer industrial waste using pollution indices and statistical techniques in the Gulf
446 of Gabes (Tunisia). *Arab J Geosci* 8: 1755-1767.
- 447 Ayadi, N., Zghal, I., Aloulou, F., Bouzid, J., 2016. Impacts of several pollutants on the
448 distribution of recent benthic foraminifera: the southern coast of Gulf of Gabes,
449 Tunisia. *Environ Sci Pollut Res* 23: 6414.
- 450 Azouazi, M., Ouahidi, Y., Fakhi, S., Andres, Y., Abbe, J. Ch., Benmansour, M., 2001.
451 Natural radioactivity in phosphates, phosphogypsum and natural waters in Morocco. *J*
452 *Environ Radioact* 54: 231-242
- 453 Batisse, M., de Grissac, A.J., 1998. A global representative system of marine protected areas.
454 *Mar. Reg. 3 Mediterr. World Bank Int. Union Conserv. Nat Nat Resour* 1: 87
- 455 Bawa, M.L., Djaneye-Boundjou, G., Boukari Y., 2006. Caractérisation de deux effluents
456 industriels au Togo: étude d'impact sur l'environnement. *Afrique Science* 2: 57-68.
- 457 Ben Hassen, A., Trichet, J., Disnar, J.R., Belayouni, H., 2010. Pétrographie et géochimie
458 comparées des pellets phosphatés et de leur gangue dans le gisement phosphaté de
459 Ras-Draâ (Tunisie). Implications sur la genèse des pellets phosphatés. *Swiss J.*
460 *Geosci.* 103:457-473.
- 461 Bolívar, J.P., Garcia-Tenorio, R., Mas, J., 1998. Radioactivity of phosphogypsum in the
462 southwest of Spain, *Radiat. Protect Dosim* 76: 185-189.

463 Chiffolleau, J.F., Claisse, D., Cossa, D., Ficht, A., Gonzalez, J.L., Guyot, T., Michel, P.,
464 Miramand, P., Oger, C., Petit, F., 2001. La contamination métallique. Programme
465 Seine Aval, fascicule n°8, Editions Ifremer, Plouzané (France). ISBN 2-84433-028-2,
466 39 p.

467 Darmoul, B., 1988. Pollution dans le Golfe de Gabès (Tunisie) : bilan des six années de
468 surveillance (1976-1981). Bull Inst Nat Sci Technol Mer Salammbô 15: 61-84

469 Darmoul, B., Hadj Ali Salem, M., Vitiello, P., 1980. Effets des rejets industriels de la région
470 de Gabès sur le milieu récepteur. Bull Inst Nat Sci Technol Mer Salammbô 7: 5-61

471 Darmoul, B., Vitiello, P., 1980. Recherches expérimentales sur la toxicité aiguë des rejets de
472 phosphogypse sur quelques organismes benthiques marins. Bull Inst Nat Sci Technol
473 Mer Salammbô 7: 63-89.

474 De Gaillande, D., 1970. Note sur les peuplements de la zone centrale du Golfe de Gabès
475 (campagne Calypso 1965). Téthys 2: 131-138

476 El Kateb, A., Stalder, C., Neururer, C., Pisapia, C., Spezzaferri, S., 2016. Correlation between
477 pollution and decline of Scleractinian *Cladocora caespitosa* (Linnaeus, 1758) in the
478 Gulf of Gabes. Heliyon 2, e00195.

479 El Kateb, A., Stalder, C., Rüggeberg, A., Neururer, C., Spangenberg, J. E., Spezzaferri, S.,
480 2018. Impact of industrial phosphate waste discharge on the marine environment in
481 the Gulf of Gabes (Tunisia). Plos One, doi.org/10.1371/journal.pone.0197731

482 El Zrelli, R., Courjault-Radé, P., Rabaoui, L., Castet, S., Michel, S., Bejaoui, N., 2015. Heavy
483 metal contamination and ecological risk assessment in the surface
484 sediments of the coastal area surrounding the industrial complex of Gabes city Gulf
485 of Gabes, SE Tunisia. Mar Poll Bull 101: 922-929

486 El Zrelli, R., Courjault-Radé, P., Rabaoui, L., Daghbouj, N., Mansour, L., Balti, R., Castet, S.,
487 Attia, F., Michel, S., Bejaoui, N., 2017. Biomonitoring of coastal pollution in the Gulf
488 of Gabes (SE, Tunisia): use of *Posidonia oceanica* seagrass as a bioindicator and its
489 mat as an archive of coastal metallic contamination. Environ Sci Pollut Res 24:
490 22214–22225

491 El Zrelli, R., Rabaoui, L., Ben Alaya, M., Daghbouj, N., Castet, S., Besson, P., Michel, S.,
492 Bejaoui, N., Courjault-Radé, P., 2018a. Seawater quality assessment and identification
493 of pollution sources along the central coastal area of Gabes Gulf (SE Tunisia):
494 Evidence of industrial impact and implications for marine environment protection.
495 Mar Poll Bull 127: 445-452

496 El Zrelli, R., Rabaoui, L., Daghbouj, N., Abda, H., Castet, S., Josse, C., van Beek, P.,
497 Souhaut, M., Michel, S., Bejaoui, N., Courjault-Radé, P., 2018b. Characterization of
498 phosphate rock and phosphogypsum from Gabes phosphate fertilizer factories (SE
499 Tunisia): high mining potential and implications for environmental protection. Environ
500 Sci Poll Res 25(15):14690-14702.

501 El Zrelli, R., Rabaoui, L., Abda, H., Daghbouj, N., Pérez-López, R., Castet, S., Aigouy, T.,
502 Bejaoui, N., Courjault-Radé, P., 2019. Characterization of the role of phosphogypsum
503 foam in the transport of metals and radionuclides in the Southern Mediterranean Sea. J
504 Hazard Mater 363: 258-267.

505 Fakhri, M., Abboud-Abi Saab, M., Romano, J.C., Mouawad, R., 2009. Impact of phosphate
506 factory on the biological characteristics of North Lebanon surface sediments
507 (Levantine Basin), Hal-00357034. 11 p.

508 Fakhri, M., Abboud-Abi Saab, M., Romano, J.C., 2008. The use of sediments to assess the
509 impact of Selaata phosphate plant on Batroun coastal area (Lebanon, Levantine Basin).
510 Lebanese Science Journal 9: 29-42.

511 Fakhri, M., Khalaf, G., Abboud-Abi Saab, M., Mouawad, R., Abi Chahine, C., Hamzé, M.,
512 2011. Résultats préliminaires de l'impact des rejets d'une usine
513 chimique sur l'environnement marin pélagique et benthique de la côte
514 libanaise. Lebanese Science Journal 12 (2): 33-44.

515 Gargouri, D., Azri, C., Serbaji, M.M., Jedoui, Y., Montacer, M., 2011. Heavy metal
516 concentrations in the surface marine sediments of Sfax Coast, Tunisia. Environ Monit
517 Assess 175: 519-530.

518 Gaudry, A., Zeroual, S., Gaie-Levrel, F., Moskura, M., Boujrhal, F.Z., El Moursli, R.C.,
519 Guessous A., Mouradi, A., Givernaud, T., Delmas, R., 2007. Heavy metals pollution
520 of the Atlantic marine environment by the Moroccan phosphate industry, as observed
521 through their bioaccumulation in *Ulva Lactuca*. Water Air Soil Pollut 178: 267-285.

522 Gezer, F., Turhan, S., Ugur, F.A., Goren, E., Kurt, M.Z., Ufuktepe, Y., 2012. Natural
523 radionuclide content of disposed phosphogypsum as TENORM produced from
524 phosphorus fertilizer industry in Turkey. Ann Nucl Ener 50: 33–37.

525 Groeneveld, R.A., Bartelings, H., Börger, T., Bosello, F., Buisman, E., Delpiazzo, E., Eboli,
526 F., Fernandes, J.A., Hamon, K.G., Hattam, C., Loureiro, M., Nunes, P.A.L.D.,
527 Piwowarczyk, J., Schasfoort, F.E., Simons, S.L., Walker, A.N., 2018. Economic

528 impacts of marine ecological change: review and recent contributions of the
529 VECTORS project on European marine waters. *Estuar Coast Shelf Sci* 201: 152-163.

530 Guillaumont, B., Ben Mustapha, S., Ben Moussa, H., Zaouali, J., Soussi, N., Ben Mammou,
531 A., Cariou C., 1995. Pollution impact study in Gabes Gulf (Tunisia) using remote
532 sensing data. *Mar Technol Soc J* 29: 46-58.

533 Gzam, M., Mejdoub, N.E., Jedoui, Y., 2016. Late quaternary sea level changes of Gabes
534 coastal plain and shelf: Identification of the MIS 5c and MIS 5a onshore highstands,
535 southern Mediterranean. *J Earth Syst Sci* 125: 13-28.

536 Halouani, G., Abdou, K., Hattab, T., Romdhane, M.S., Lasram, F.B.R., Le Loc'h, F., 2016. A
537 spatio-temporal ecosystem model to stimulate fishing management plans: a case study
538 in the Gulf of Gabes (Tunisia). *Mar Pol* 69: 62-72

539 Hattab, T., Lasram, F.B.R., Albouy, C., Romdhane, M.S., Jarboui, O., Halouani, G., Cury, P.,
540 Le Loc'h, F., 2013. An ecosystem model of an exploited southern Mediterranean shelf
541 region (Gulf of Gabes, Tunisia) and a comparison with other Mediterranean ecosystem
542 model properties. *J Mar Sys* 128: 159-174

543 Hattour, A., Ben Mustapha, K., 2013. Le couvert végétal marin du golfe de Gabès :
544 Cartographie et réseau de surveillance de l'herbier de Posidonie. *Publ Inst Natn Sci*
545 *Tech Mer* 151 p.

546 Hattour, M.J., Sammari, C., Ben Nassrallah, S., 2010. Hydrodynamique du golfe de Gabès
547 déduite à partir des observations de courants et de niveaux. *Rev Paralia* 3: 1-12.

548 Kindt, J.W., 1984. Solid wastes and marine pollution. *Cath. U. L. Rev.* 34: 37-100.

549 Maggi, P., 1973. Le problème de la disparition des herbiers à posidonies dans le Golfe de
550 Giens (Var). *Science et Pêche. Bull Inst Pêches Marit* (221): 7-20.

551 METAP/Tebodin, 1998. Ministry of Environment. Industrial pollution control Lebanon.
552 Prepared by Tebodine and financed by the World Bank and UNIDO.

553 Morillo, J., Usero, J., Gracia, I., 2004. Heavy metal distribution in marine sediments from the
554 southwest coast of Spain. *Chemosphere* 55: 431-442.

555 Naifar, I., Pereira, F., Zmemla, R., Bouaziz, M., Elleuch, B., Garcia, D., 2018. Spatial
556 distribution and contamination assessment of heavy metals in marine sediments of the
557 southern coast of Sfax, Gabes Gulf, Tunisia. *Mar Poll Bull* 131 : 53-62.

558 Newman, S., Watkins, E., Farmer, A., ten Brink, P., Schweitzer, J.P., 2015. The economics of
559 marine litter. In: Bergmann M, Gutow L, Klages M (Eds), *Marine Anthropogenic*
560 *Litter*. Springer, Berlin pp 367-394

- 561 Papaconstantinou, C., Farrugio, H., 2000. Fisheries in the Mediterranean. *Med Mar Sci* 1: 5-
562 18.
- 563 Papageorgiou, F., Godelitsas, A., Mertzimekis, T.J., Xanthos, S., Voulgaris, N., Katsantonis,
564 G., 2016. Environmental impact of phosphogypsum stockpile in remediated Schistos
565 waste site (Piraeus, Greece) using a combination of γ -ray spectrometry with
566 geographic information systems. *Environ Monit Assess* 188: 133
- 567 Pérez-López, R., Castillo, J., Sarmiento, A.M., Nieto, J.M., 2011. Assessment of
568 phosphogypsum impact on the salt-marshes of the Tinto River (SW Spain): role of
569 natural attenuation processes. *Mar Poll Bull* 62: 2787-2796.
- 570 Periañez, R., 2002. The enhancement of ^{226}Ra in a tidal estuary due to the operation of
571 fertilizer factories and redissolution from sediments: experimental results and a
572 modelling study. *Estuar Coast Shelf Sci* 54: 809-819.
- 573 Poizat, C., 1970. Hydrodynamisme et sédimentation dans le golfe de Gabès (Tunisie). *Téthys*
574 2 (1) : 267-296.
- 575 Rabaoui, L., Balti, R., El Zrelli, R., Tlig-Zouari, S., 2014. Assessment of heavy metals
576 pollution in the gulf of Gabes (Tunisia) using four mollusk species. *Mediterr Mar Sci*
577 15: 45-58
- 578 Rabaoui, L., El Zrelli, R., Balti, R., Mansour, L., Courjault-Radé, P., Daghbouj, N., Tlig-
579 Zouari, S., 2017. Metal bioaccumulation in two edible cephalopods in the Gulf of
580 Gabes, South-Eastern Tunisia: environmental and human health risk assessment.
581 *Environ Sci Poll Res* 24 (2): 1686-1699
- 582 Rabaoui, L., El Zrelli, R., Ben Mansour, M., Balti, R., Mansour, L., Tlig-Zouari, S., Guerfel,
583 M., 2015. On the relationship between the diversity and structure of benthic
584 macroinvertebrate communities and sediment enrichment with heavy metals in Gabes
585 gulf Tunisia. *J Mar Biol Assoc UK* 95: 233-245
- 586 Rabaoui, L., Tlig-Zouari, S., Katsanevakis, S., Ben Hassine, O.K., 2010. Modelling
587 population density of *Pinna nobilis* (Bivalvia) on the eastern and southeastern coast of
588 Tunisia. *J Moll Stud* 67: 340-347
- 589 Sassi, A.B., Sassi, S., 1999. Le cadmium associé aux dépôts phosphatés en Tunisie
590 Méridionale. *J Afr Sci* 29: 501-513
- 591 Seurat, L.G., 1934. Formations littorales et estuaires de la Syrte mineure (Golfe de Gabès).
592 *Bull. Stat. Océanogr. Salammbô* 32: 1-65

593 Simon, S., Elkaim, B., Chouquet, B., 2000. Rapport annuel sur la surveillance de la faune
594 benthique à proximité des rejets de phosphogypses en estuaire de Seine. Rapport
595 technique n° 60, Commission chargée de contrôler l'évolution de la pollution en
596 Estuaire et en Baie de Seine: Le Havre, 45 p.

597 Tayibi, H., Choura, M., López, F.A., Alguacil, F.J., López-Delgado, A., (2009. Environmental
598 impact and management of phosphogypsum. J Environ Manag 90 (8): 2377-2386

599 Totic, M., Restrepo, J.D., Izquierdo, A., Lonin, S., Martins, F., Escobar, R., 2018. An
600 integrated approach for the assessment of land-based pollution loads in the coastal
601 zone. Estuar Coast Shelf Sci 211 : 217-226.

602 UNEP (The United Nations Environment Program), 2012. État de l'environnement marin et
603 côtier de la Méditerranée–Convention de Barcelone, Athènes.

604 Wilcock, P., Pitlick, J., Cui, Y., 2009. Sediment transport primer: Estimating bed-material
605 transport in gravel-bed rivers. Rocky Mountain Research Station: U.S. Department of
606 Agriculture Available from: General Technical Report RMRS-GTR-22.

607 Zaouali, J., 1993. Les peuplements benthiques de la petite Syrte, golfe de Gabès- Tunisie.
608 Résultats de la campagne de prospection du mois de juillet 1996. Étude préliminaire :
609 biocénoses et thanatocénoses récentes. Mar Life 3: 47-60.


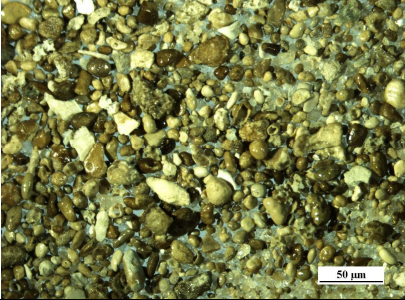



610

Table 1. Table summarizing the locations and number of trenches realized in each sampling station and in each sector, number and labels of sediments layers observed and number of samples collected from layers/trenches.

Sectors	Trenches	Latitude	Longitude	Layers	Number of samples
Inter-harbor Sector	LG	33.913183	10.103017	L4	2
	CE	CE1	10.109032	L1, L2 and L3	3
		CE2	10.109278	L1, L2 and L3	3
Southern Sector	CE3	33.900501	10.109706	L4	2
	CR	33.888367	10.119399	L1 and Ls	2
		OG	33.881070		10.123885
	CM	33.872555	10.131456		2
	MT	33.866872	10.136622		2
	TB	33.856182	10.147702		2
Zone 2	LM	33.830594	10.175549		L1
	KT	33.791923	10.229626	L1	1
		ZT	33.713848		10.326283

615 **Table 2.** Description of different coastal layers. (Ls: G×15; L4: G×10; L3: G×15; L2: G×20;
 616 L1: G×20).

617

Layers	Binocular loupe photo	Description
L _s		<p>Color: greyish Composition: Quartz, calcite, zircon, titanomagnetite, Calcite-Mg and small spherical shape fluorapatite grains (Ø<250µm), with a homogeneous fine granulometry. Spatial extension: in the southern area, from Corniche to Tebelbou (Sourrag Wadi).</p>
L4		<p>Color: Dark brown to blackish Composition: Almost dominance of fluorapatite grains, with the presence of smokey quartz grains, sphalerite-Cd, calcite-Mg, feldspar-K, fluorosilicates, sulfur dross and spent catalysts, with a very coarse heterogeneous granulometry. Spatial extension: in the inter-harbor area.</p>
L3		<p>Color: Brown Composition: Fluorapatite, quartz, calcite, zircon, calcite-Mg, sphalerite-Cd with the minority presence of barite and albite with heterogeneous medium granulometry. Spatial extension: in the inter-harbor area.</p>
L2		<p>Color: greyish Composition: Quartz, calcite, calcite-Mg, fluorapatite, zircon, fluorite, apatite and titanomagnetite, with a homogeneous medium to fine granulometry. Spatial extension: in the inter-harbor area.</p>
L1		<p>Color: white to blond yellowish Composition: Quartz grains, calcite grains (fragments of shells) and opaque grains (zircon, iron oxides and titanomagnetite minerals), with a homogeneous fine granulometry. Spatial extension: from Chatt Essalam to Zarat.</p>

618

Figures Captions

619
620
621
622
623
624
625
626
627
628
629
630
631
632
633
634
635
636
637
638
639
640
641

Fig. 1. Location of the study area and sampling stations.

Fig. 2. Mineralogical composition of the sediment samples collected from the bed of the marine industrial discharges of the Gabes phosphate chemical complex (1: fluorapatite, 2: smokey Quartz, 3: calcite, 4: used catalysts, 5: sulfur dross, 6: sphalerite-Cd-U (+ fluorite), 7: apatite, 8: fluorosilicates. All the minerals presented here (1-8) were found in different samples and combined together just to show the mineralogical composition of these samples.

Fig. 3. SEM image and EDS spectra of Sphalerite-Cd-U.

Fig. 4. Sequential organization of L1, L2, L3, L4 and L_s layers at Gabes Beach. A and B at Chatt Essalam Beach, and C at M'torrech station (zone1).

Fig. 5. North-South (N-S) sedimentary organization of the study beach area.

Fig. 6. Variations of Pb, Cd, Zn, Cr, Cu, Hg (in mg kg⁻¹) and P_{ing} (in g kg⁻¹) concentration (log-transformed) among the four different sediment layers observed and samples in Chat Essalam Beach.

Fig. 7. SEM photos of (A) representative fluorapatite mineral grains from Legusir (LG), Chatt Essalam (CE) (Zone 1) and Tebelbou (TB) (Zone 2) stations and

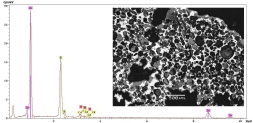


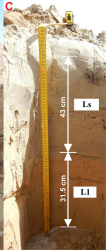
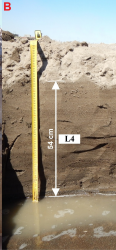
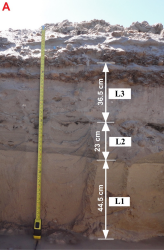
Gulf of Gabes



1 cm







LG



200 μ m

CE

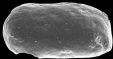


200 μ m

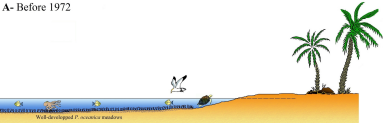
TB



200 μ m



A- Before 1972



B- After 1972

The main coastal changes caused by industrial solid wastes are: local extinction of *Posidonia oceanica*, installation of azoic benthic seabed in the inter-harbor area, gradual fattening of beaches, advancement of the shoreline, clogging of the coastal rivers mouths and formation of coastal lakes.

